# MedChemComm

Accepted Manuscript



This is an *Accepted Manuscript*, which has been through the Royal Society of Chemistry peer review process and has been accepted for publication.

Accepted Manuscripts are published online shortly after acceptance, before technical editing, formatting and proof reading. Using this free service, authors can make their results available to the community, in citable form, before we publish the edited article. We will replace this Accepted Manuscript with the edited and formatted Advance Article as soon as it is available.

You can find more information about *Accepted Manuscripts* in the **Information for Authors**.

Please note that technical editing may introduce minor changes to the text and/or graphics, which may alter content. The journal's standard <u>Terms & Conditions</u> and the <u>Ethical guidelines</u> still apply. In no event shall the Royal Society of Chemistry be held responsible for any errors or omissions in this *Accepted Manuscript* or any consequences arising from the use of any information it contains.



## Novel indole-flutimide heterocycles with activity against influenza PA endonuclease and hepatitis C virus

Grigoris Zoidis,\*,<sup>a</sup> Erofili Giannakopoulou,<sup>a</sup> Annelies Stevaert,<sup>b</sup> Efseveia Frakolaki,<sup>c</sup> Vassilios Myrianthopoulos,<sup>a</sup> George Fytas,<sup>a</sup> Penelope Mavromara,<sup>c</sup> Emmanuel Mikros,<sup>a</sup> Ralf Bartenschlager,<sup>d,e</sup> Niki Vassilaki<sup>c,†</sup> and Lieve Naesens<sup>b,§</sup>

<sup>a</sup>School of Health Sciences, Faculty of Pharmacy, Department of Pharmaceutical Chemistry, University of Athens, Panepistimioupoli-Zografou, GR-15784, Athens, Greece

<sup>b</sup>Rega Institute for Medical Research, KU Leuven – University of Leuven, B-3000 Leuven, Belgium

<sup>c</sup>Molecular Virology Laboratory, Hellenic Pasteur Institute, Vas. Sofias Avenue, 11521, Athens, Greece

<sup>d</sup>Department of Infectious Diseases, Molecular Virology, University of Heidelberg, Heidelberg, Germany

<sup>e</sup>German Center for Infection Research, Heidelberg University

## **Abstract**

Influenza viruses cause considerable morbidity and mortality, whether in the context of annual epidemics, sporadic pandemics, or outbreaks of avian influenza virus. For hepatitis C virus (HCV), an estimated 170 million people are chronically infected worldwide. These individuals are at high risk of developing progressive liver injury or hepatocellular carcinoma. Since the efficacy of currently approved antiviral drugs is threatened by emerging viral resistance and the cost remains high, new antiviral drugs are still required. By utilizing a structure-based approach, novel substituted indole-flutimide heterocyclic derivatives (1,2-annulated indolediketopiperazines) were rationally designed, synthesized and evaluated as influenza PA endonuclease inhibitors. The compounds were also tested for their antiviral effect against HCV. All

<sup>\*</sup>Corresponding author Dr. Grigoris Zoidis (zoidis@pharm.uoa.gr)

<sup>&</sup>lt;sup>†</sup>Principal investigator of the study on Hepatitis C virus

<sup>§</sup>Principal investigator of the study on influenza A endonuclease

*N*-hydroxyimides were potent PA endonuclease inhibitors while displaying low cytotoxicity. Compound **6** proved to be the most active analogue, while the most favorable indole substitution was fluorine at position 8 (compound **18**). The chloroderivative **24** showed additional potent anti-HCV activity and exhibited remarkable selectivity (>19). In accordance with the SAR data, removal of the hydroxyl group from the imidic nitrogen (compound **26**) caused a complete loss of activity against influenza PA as well as HCV.

**KEYWORDS:** Antiviral, influenza virus, endonuclease, Hepatitis C virus, HCV NS5B polymerase, NMR, indolediketopiperazines, flutimide, docking calculations, SZmap.

## Introduction

Influenza virus is a major respiratory pathogen. Worldwide, influenza affects about 120 million people per year; the number of severe cases is estimated to be between 3 and 5 million with up to 500,000 deaths. The main prophylactic measure, vaccination, requires annual updating and is only partially protective in elderly people. Also, as seen in 2009, there is a lag time of about 6 months between recognition of a new pandemic strain and availability of the vaccine. Hence, antiviral therapeutics are an important alternative. Two drug classes, targeting either the viral neuraminidase (oseltamivir and zanamivir), or M2-ion channel (adamantanes), are in clinical use, but emerging resistance can threaten their long-term efficacy. As a result, there is an immediate need for novel anti-influenza drugs.

To perform viral mRNA transcription, the influenza virus depends on a unique 'cap-snatching' reaction that is performed by the viral polymerase.<sup>8</sup> This heterotrimeric protein complex comprises the subunits PA, PB1, and PB2. During the

reaction, the PB2 subunit binds the cap at the 5'-end of host pre-mRNAs. The bound mRNA is then cleaved 10–15 nucleotides downstream, by the N-terminal domain of the PA endonuclease ( $PA_N$ ). Next, the capped 5'-oligonucleotide cleavage product functions as the primer for viral mRNA synthesis, which is catalyzed by the PB1 polymerase subunit.

The active site of the PA<sub>N</sub> endonuclease comprises a histidine and a cluster of three acidic residues, conserved in all influenza viruses, which bind one, two or possibly three divalent (manganese or magnesium) metal ions. 9, 10 PA<sub>N</sub> is an attractive antiviral target for a number of reasons<sup>11</sup>: (i) the endonuclease reaction is indispensable for virus replication. (ii) Since the PA<sub>N</sub> domain is highly conserved in all influenza A and B viruses, PA<sub>N</sub> inhibitors are expected to have broad anti-influenza virus activity with a higher barrier for selecting resistance. (iii) The lack of a  $PA_N$ human counterpart implicates that the design of highly selective, non-toxic inhibitors should be feasible. (iv) PA<sub>N</sub> inhibitors target a different enzyme than currently marketed influenza blockers, creating the potential for combination therapy to circumvent the propensity of the virus to undergo rapid mutation and adaptation. 12 (v) Finally, due to the blockade in viral transcription, endonuclease inhibition has a virucidal effect. 13 In contrast, the neuraminidase inhibitors are virustatic since they interfere with virus release from the host cells and hence, do not prevent the formation of new virus particles.

Hepatitis C virus (HCV) infection is the major cause of chronic liver disease that often leads to cirrhosis and hepatocellular carcinoma. No vaccine is currently available. The approved antivirals can cure hepatitis C in 50-90% of patients, let but access to diagnosis and treatment is low. The standard of care until recently, i.e.

pegylated IFN $\alpha$  plus ribavirin,<sup>21</sup> is only partially effective and associated with numerous side-effects. The introduction of an efficient HCV cell culture system, based on the JFH1 isolate and Huh7.5 cells,<sup>22</sup> enabled the development of promising direct acting antivirals (DAAs), which have shorter treatment duration and fewer side effects. Recently, the nucleotide analogue sofosbuvir combined with ribavirin or IFN $\alpha$ /ribavirin was approved for genotypes 1-4 with high cure rates.<sup>23</sup> Multiple IFN $\alpha$ -free DAA regimens containing HCV polymerase inhibitors are in late-stage clinical trials and expected to be approved within the next few years.<sup>24, 25</sup>

However, due to the high cost of these treatments, there is still a need for new drugs that will be affordable in low-income countries. Novel promising HCV inhibitors have been isolated from various organisms and some have already been applied to patients with chronic hepatitis C.<sup>26, 27</sup>

HCV belongs to the Flaviviridae family<sup>28</sup> and is classified into seven major HCV genotypes and more than one hundred subtypes.<sup>29</sup> The single-stranded positive-sense RNA genome of HCV encodes a polyprotein precursor, which is processed into structural proteins (core, E1 and E2), p7 required for assembly and release, and nonstructural proteins (NS2, NS3, NS4A, NS4B, NS5A and NS5B) which form a membrane-associated replicase complex in association with cellular factors.<sup>30, 31</sup> Among the non-structural proteins, NS3-4A serine-protease and NS5B viral polymerase have been the primary viral targets in the development of DAAs.

The HCV polymerase exhibits important differences with cellular polymerases, making it a relevant target for developing specific inhibitors. This RNA-dependent RNA polymerase (RdRp) catalyzes the synthesis of both negative-strand copies of the incoming viral RNA and positive-strand progeny RNA genomes.<sup>32</sup> In *in vitro* assays,

purified NS5B can initiate RNA synthesis by a primer-dependent or *de novo* mechanism. *De novo* initiation at the 3' end of the positive or negative-strand RNA is the likely physiological mode for initiation of RNA synthesis in infected cells. Similar to other known RdRps, the HCV polymerase contains six conserved motifs A-F.<sup>33</sup> In the crystal structure of HCV NS5B,<sup>33-36</sup> three domains known as palm, fingers, and thumb can be discerned. The conformation is contracted closed enough for binding of a single-stranded RNA template and the priming nucleotides. Two divalent metal ions, coordinated in the palm domain, facilitate the catalytic activity of NS5B. Both Mn<sup>2+</sup> and Mg<sup>2+</sup> can support RdRp activity in enzymatic assays.

Based on their chemical structure and/or mechanism of action, the HCV NS5B inhibitors can be classified into:<sup>37</sup> nucleoside/nucleotide analogues (including the purine analogue ribavirin); non-nucleoside allosteric inhibitors of NS5B; inhibitors that covalently change the residues near the active site of NS5B and occasionally act by chelating the divalent metal ions needed by NS5B; and finally compounds that target cellular proteins needed for NS5B function.

In the present study, a series of flutimide analogues, specifically novel lipophilic 1,2-annulated indole diketopiperazines, were rationally developed. The compounds were assessed as inhibitors of influenza PA endonuclease and HCV polymerase, since these two enzymes demonstrate resemblance with respect to their active sites dependence on two divalent metal ions. Warious substituents such as hydroxy-, methoxy-, chloro- and fluoro-groups were introduced into the core structure, and all analogues were evaluated for their inhibitory effect on the influenza PA endonuclease and HCV RNA replication in the subgenomic replicon assay.

## **Results and Discussion**

## Theoretical calculations and rational design

A number of PA inhibitors with a metal-chelating functional group have been published. For instance, a core consisting of *N*-hydroxyimide or dioxobutanoic acid is present in the prototype inhibitors flutimide<sup>39</sup> and 2,4-dioxo-4-phenylbutanoic acid<sup>40</sup> (DPBA), respectively. Flutimide, a fully substituted 1-hydroxy-3*H*-pyrazine-2,6-dione (Figure 1), was originally isolated from the fungus *Delitschia confertaspora*. This compound was reported to selectively inhibit the cap-dependent endonuclease reaction of influenza A and B viruses, most likely by chelating the two divalent metal ions (Mn<sup>2+</sup> and/or Mg<sup>2+</sup>) in the PA<sub>N</sub> active site.<sup>39, 41</sup> In addition, *N*-hydroxyimides that are structurally related to flutimide have been reported as potent inhibitors of HIV ribonuclease H (RNH)<sup>42</sup> or HIV integrase (IN).<sup>43</sup> A commonality among PA<sub>N</sub>, RNH, HIV IN and HCV NS5B polymerase<sup>44</sup> is the presence of two divalent metal ions in the active site, which implicates that a basic metal-chelating pharmacophore might be amended to achieve activity against one or more of these enzymes.

The other compound, DPBA, is an aromatic compound with a 2,4-dioxobutanoic side chain. This molecule is a well-known inhibitor of the influenza virus endonuclease reaction,<sup>40, 45</sup> which however has no activity in cell culture due to its low cell permeability, thus limiting its drug-like properties.

I (Flutimide : 
$$5.5 \,\mu\text{M}$$
) II (DPBA :  $5.4 \,\mu\text{M}$ ) III Novel Flutimide analogues (X : H, CI, F, CH<sub>3</sub>O, OH)

**VIII** (> 500 μM)

IX (> 500 µM)

X (25% @ 100 µM)

VI (800 µM) VII (95 µM) Figure 1. Flutimide, DPBA, and diverse flutimide and N-hydroxyimide analogues with inhibitory activity against influenza endonuclease. Numbers in brackets denote the IC50 values reported in the literature and determined in the cap-dependent RNA polymerase assay with influenza A polymerase. <sup>39, 40, 46, 47</sup> Class III are the flutimide analogues reported in the present study.

To gain insight into the SAR for PA<sub>N</sub> inhibition and suggest possible chemical modifications for optimization of the available leads, molecular simulations were undertaken. The results of modeling studies were utilized to rationally conceive a series of structural changes that would potentially enhance binding affinity and improve drug-likeness of the available inhibitors. To this end, the drug-like core structure of indole was selected to be introduced to the 2,6-diketopiperazine scaffold of flutimide (Figure 1). Indole represents one of the most versatile structural motifs in drug discovery, which is capable of serving as ligand for a diverse array of receptors by mimicking the structure of peptides and binding reversibly to enzymes, providing tremendous opportunities for drug discovery. During the last decades, indole derivatives have attracted considerable attention, as evidenced by the fact that seven indole-containing drugs are among the top-200 best-selling drugs by US Retail Sales in 2012.<sup>48</sup> Moreover, given the mechanistic similarity between influenza PA<sub>N</sub> endonuclease and HCV NS5B polymerase, the novel flutimide heterocyclic

analogues could possibly be active inhibitors towards HCV as well. Indeed, metal-chelating structurally related derivatives including hydroxy-isoquinoline-diones have been already identified to inhibit HCV NS5B.<sup>43</sup>

A small number of complexes of the protein with various inhibitors such as DPBA are currently available, providing basic SAR insight to the interaction mode of those molecules with the enzyme. 41, 49, 50 Inspection of the structures revealed that the major stabilizing interactions of the PA-inhibitor complexes are electrostatic in nature and primarily formed between the chelating moiety of the ligands and the highly polar catalytic region of the enzyme. In each case, strong ionic interactions along with charge-assisted hydrogen bonds anchor the chelator moiety of DPBA to the PA catalytic ensemble comprised by the two positively charged Mn<sup>2+</sup> ions and residues Glu80, Asp108, Glu119, Lys134 and His41 (Figure 2a). A comparative inspection of the binding modes of the reference compound DPBA (pdb id: 4AWF) and complexes with derivatives of 3-hydroxyguinolin-2-one<sup>49</sup> (pdb id: 4KIL) and 3hydroxypyridin-2-one<sup>50</sup> (pdb id: 4M5U) suggested possible directions towards which the novel flutimide-derived indole-containing scaffold could be extended, aimed at enhancing the stabilizing interactions with the target enzyme. Initial extension of novel scaffold was performed along the vector pointing from the metal-chelating pharmacophore towards the N-terminal side of the PA pocket, as indicated in Figure 2a (green arrow) by replacing the 2-oxobutanoic group of the lead DPBA by an Nhydroxyimidic moiety and as already mentioned, by incorporating an indole at the opposite with respect to the pharmacophore side. Moreover, a secondary cavity adjacent to the PA active site in the vicinity of the N-terminal region was additionally targeted. This cavity is formed by residues Met21, Tyr24, Glu26, Lys34 and Ile38 and

is also exploited by 3-hydroxyquinolin-2-ones and 3-hydroxypyridin-2-ones, as evidently shown in the respective complexes. 49, 50. Despite its moderate polar character, an active site hydration analysis performed by implementing SZmap algorithm demonstrated that this cavity is rather poorly hydrated. 51 More specifically, a small cluster of moderately unstable water molecules were identified, with SZmap-calculated free energies ranging from +1.05 to +1.30 Kcal/mol. This observation thus offered additional opportunities for probing possible enhancement of inhibitor binding affinity by indole substitutions which could interfere with the abovementioned structural waters. Such substitutions could displace unstable solvent molecules, giving rise to affinity gain through favorable entropic contributions.

To gain additional insight to the binding mode of the novel analogues, docking calculations were undertaken utilizing Glide software. 52-55 In the absence of a crystallographic structure of flutimide in complex with the PA endonuclease, its complex with the relatively small DPBA molecule was finally utilized for calculations. This selection was regarded as a means to avoid modeling bias arising from possible induced-fit effects on the other available endonuclease structures due to the bulkiness of 3-hydroxyquinolin-2-one and 3-hydroxypyridin-2-one cocrystallized ligands. Docking calculations on the designed analogues showed that all ionic interactions between DPBA and the protein were perfectly retained, well justifying for selection of the isosteric *N*-hydroxyimidic moiety and its enhanced drug-like properties in terms of lipophilicity and pK<sub>a</sub> with respect to the 2-oxobutanoic group (Table 1). At the same time, the extended aromatic system of the novel analogues facilitated considerable hydrophobic as well as stacking interactions with the protein

and more specifically with the sidechains of Tyr24, Lys34 and Ile38. Notably, docking results showed that the binding orientation of the indole system within the cavity further assisted correct positioning of the scaffold core substitutions at position 8 as designed, towards the aforementioned N-terminal cavity and the unstable water molecules (Figure 2A). The encouraging results obtained by docking calculations prompted the chemical synthesis of the compounds and their subsequent evaluation in biological assays.

## Chemistry

Scheme 1. Synthesis of the target 1,2-annulated indole heterocycles 6, 12, 18, 25 and 26.

Scheme 2. Synthesis of the target 1,2-annulated indole heterocycle 24.

As depicted in Schemes 1 and 2, carboxylic acids 4, 10, 16 and 22 were the key structures to prepare the new target compounds and were synthesized from the respective, commercially available, 5-substituted-1H-indole-2-carboxylic acids. The latter compounds were esterified either with benzyl alcohol (Scheme 1) or with 4methoxybenzyl alcohol (Scheme 2) in the presence of 4-(dimethylamino)pyridine (DMAP) and N,N'-dicyclohexylcarbodiimide (DDC) in dichloromethane. 56 Benzyl indole-2-carboxylates are converted to the corresponding diesters 3, 9, 15 and 21 upon reaction with ethylbromoacetate in the presence of sodium hydride in DMF. Deprotection of the latters, either with hydrogenolysis (Pd/C 10%) or with trifluoroacetic acid (TFA) in the presence of anisole (methoxybenzene) as a scavenger, yielded, in almost quantitative yield, the key intermediates 5-substituted-1-(2-ethoxy-2-oxoethyl)-1H-indole-2-carboxylic acids 4, 10, 16 and 22. Their coupling with O-benzyl or O-4-methoxybenzyl hydroxylamine in the presence of EDCI·HCl, HOBt in CH<sub>2</sub>Cl<sub>2</sub>/DMF led to the corresponding O-benzyl or O-4-methoxybenzyl hydroxamates which intramolecular cyclized in the presence of diisopropylethylamine (excess), in one pot, to the corresponding diketopiperazine

analogues **5**, **11**, **17** and **23** in high yields (59-80%, two steps). Finally, the protecting group was removed upon hydrogenolysis (Pd/C 10%) or in the presence of TFA/anisole to give the respective hydroxyimide analogues **6**, **12**, **18** and **24** in almost quantitative yield. The target compound **25** was synthesized by demethylation of the methylarylether **12** with the use of boron tribromide (Scheme 1).

Pyrazino[1,2-a]indole-1,3(2H,4H)-dione **26** was synthesized, as illustrated in Scheme 1, by subsequent amidation of acid-ester **4**, *via* the respective chloride, with thionyl chloride and gas NH<sub>3</sub>, and intramolecular cyclization of the intermediate amide in one pot and excellent overall yield.

## **Biology**

## **Influenza Endonuclease Assays**

<b>Table 1.</b> Inhibitory activities of novel compounds against influenza endonuclease <sup>a</sup> and HCV replication. Cytotoxicity towards Huh5-2 replicon cells and HEK293T cells and theoretical logD and $pK_a$ values for the tested compounds.										
X O N-R										
Cpd	х	R	PA endonuclease	Influenza virus vRNP assay		Hepatitis C virus			logD	p <i>K</i> <sub>a</sub>
			IC <sub>50</sub> <sup>b</sup>	EC <sub>50</sub> <sup>d</sup>	$MCC^d$	EC <sub>50</sub> <sup>e</sup>	LC <sub>50</sub> e	SI <sup>f</sup>		
Data in μM										
6	Н	ОН	12.7	297	≥500	126.3 ± 14.2	>200	>1.6	0.57	7.27
12	OCH <sub>3</sub>	ОН	23.0	48	≥500	>200	>200	-	0.41	7.27
18	F	ОН	17.3	>500	≥500	83.8 ± 4.8	>200	>2.4	0.71	7.27
24	Cl	ОН	26.9	114	≥500	10.5 ± 3.1	>200	>19.1	1.17	7.27
25	ОН	ОН	29.2	75	≥500	>200	>200	-	0.26	7.27
26	Н	Н	>500	N.D.	N.D.	>200	>200	-	0.75	9.30
DPBA <sup>c</sup>	-	-	5.4	N.D.	N.D.	>200	>200	-	-1.73	2.85

The data presented in Table 1 indicate that all compounds except **26** elicit significant inhibitory activity against influenza PA endonuclease in an enzymatic assay, with IC<sub>50</sub> values comparable with that of the reference inhibitor DPBA. The compounds were also evaluated in a cell-based influenza vRNP reconstitution assay,<sup>57</sup> in which the inhibitory effect on viral polymerase activity is measured in HEK293T cells (Table 1). Neither of the compounds produced cytotoxicity at the highest concentration tested (500  $\mu$ M). Interestingly, some inhibition of influenza polymerase activity was observed, the order of inhibitory activity being: **12** > **25** > **24** > **6**. Compound **18** was found to be inactive. Although the EC<sub>50</sub> values were relatively high, these findings present proof-of-concept evidence that the scaffold that we designed is valid for the development of novel influenza endonuclease inhibitors.

The enzymatic data with the synthesized analogues showed that the most active PA endonuclease inhibitor was compound **6** with an IC<sub>50</sub> of 12.7  $\mu$ M, while the most favorable indole substitution was fluorine at position 8 (compound **18** with an IC<sub>50</sub> of 17.3  $\mu$ M). This SAR notion was in good accordance with previous studies demonstrating that the fluorine substitution generally enhances the inhibitory activity of several chelator scaffolds.<sup>49, 50</sup> Indeed, on the basis of the determined binding affinities, fluorine seems to be more preferable than bulkier halogens. This can possibly be explained in terms of optimal Van der Waals interactions specifically with the secondary N-terminal cavity of the PA active site combined with overall balanced steric interactions with the protein. On the other hand, docking suggested

<sup>&</sup>lt;sup>o</sup>The reaction mixture contained 2 μg recombinant PA-Nter; 1 μg (16.7 nM) single stran ded circular DNA plasmid (M13mp18); buffer (50 mM Tris.HCl pH 8, 100 mM NaCl, 1 mM MnCl<sub>2</sub>, 10 mM β-mercaptoethanol); and the test compounds. After 2 h incubation at 37 °C, the endonucleolytic digestion of the plasmid was visualized by gel electrophoresis with ethidium bromide staining. <sup>45</sup>

 $<sup>^</sup>b$ IC $_{50}$  value calculated from data from three independent experiments, by non-linear regression analysis using Graphpad Prism

 $<sup>^{</sup>c}$ 2,4-Dioxo-4-phenylbutanoic acid (DPBA), a known PA $_{N}$  inhibitor, was used as a reference compound.

<sup>&</sup>lt;sup>d</sup>The EC $_{50}$  represents the compound concentration that produces 50% inhibition of influenza polymerase assay in the vRNP reconstitution assay in HEK293T cells. <sup>57</sup> The MCC is the minimum cytotoxic concentration, as determined by microscopic analysis of cell morphology. <sup>6</sup>EC $_{50}$  (concentration required for 50% inhibition of HCV replication) and LC $_{50}$  (median lethal concentration against Huh5-2, HCV replicon cells) values represent the mean  $\pm$  SD of three independent experiments, each carried out in triplicate. 
<sup>1</sup>Selectivity index: LC $_{50}$ /EC $_{50}$ .

that both fluorine and chlorine can efficaciously displace the small cluster of highenergy water molecules identified by SZmap hydration analysis (Figure 2A). Removal of such unstable solvent molecules would give rise to a moderately favorable entropic affinity gain which, albeit moderate, when combined with the low desolvation penalty, improved lipophilicity,  $pK_a$  and overall drug-likeness of **18**, could account for the promising biological activity of this analogue. Finally, the lack of inhibitory activity for compound **26** was expected since the *N*-hydroxyimide group is a prerequisite for the chelation of the metal ions inside the active site of PA endonuclease.

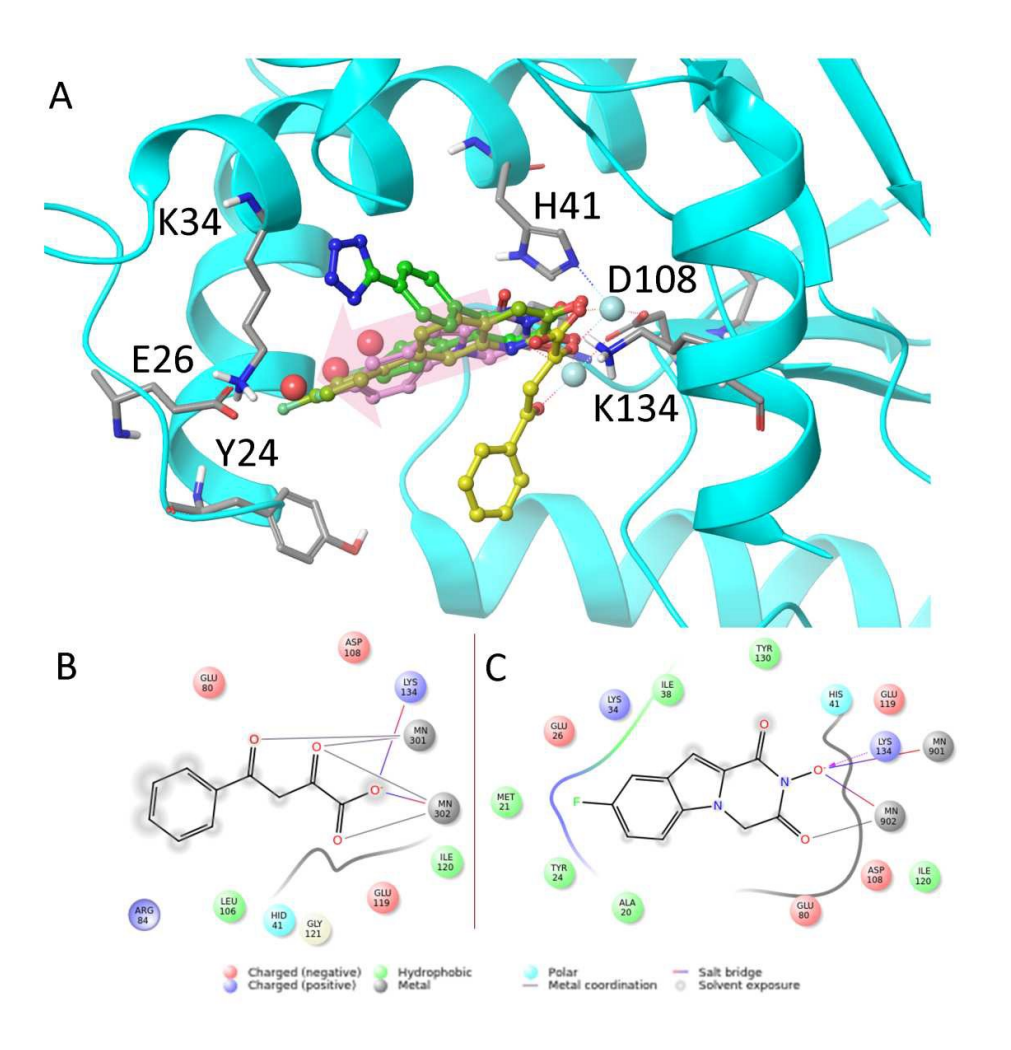
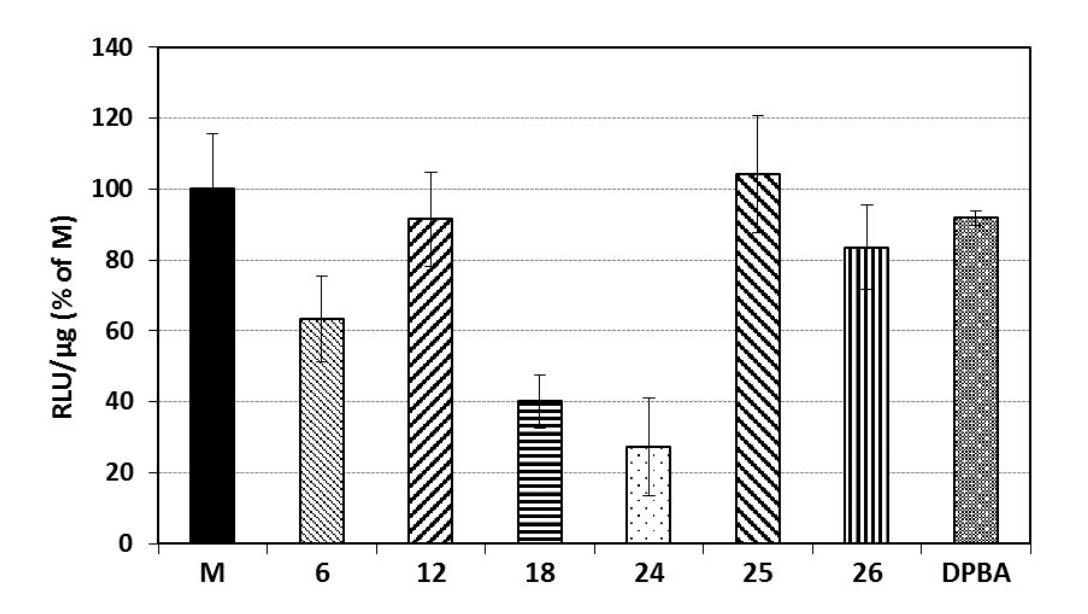


Figure 2. A) The experimental binding mode of DPBA (yellow green carbons), 3-hydroxyquinolin-2-one (light green carbons) and 3-hydroxypyridin-2-one (green carbons) inhibitors overlaid with the predicted binding mode of the novel fluoro-derivative 18 (plum carbons) in the active site of PA influenza endonuclease shown in a ribbon representation. Residues involved in inhibitor binding are depicted in a stick representation. The two manganese ions coordinated in the active site are depicted as blue opaque spheres. The three red spheres define hydration sites of high free energy and thus unstable, as determined by SZmap analysis. On the basis of the experimentally available binding modes, it was hypothesized that an extension of the novel scaffold towards the N-terminal region of PA active site would be permitted. The extension vector followed in this study is indicated as a semitransparent plum arrow. Indeed, binding of 18 demonstrated its enhanced capabilities of accommodating stacking and hydrophobic interactions with respect to DPBA. Interestingly, the inhibitor is oriented in a manner which positions the 8-substituent towards the N-terminal cavity, offering thus further possibilities for additional stabilizing interactions in a similar manner as 3hydroxyquinolin-2-ones and 3-hydroxypyridin-2-ones. Moreover, the 8-substituent of indole overlaps with the aforementioned cluster of high-energy hydration sites, thus permitting displacement of unstable waters and leading to fair affinity improvement due to favorable entropic contributions. B) Two-dimensional representation of the interactions formed between DPBA and PA endonuclease. C) Two-dimensional representation of the interactions formed between 18 and PA endonuclease.

## **HCV Replication assays**

The already mentioned similar properties of PA endonuclease and HCV polymerase in terms of two-metal ion dependence and pharmacophore requirements, prompted experimental evaluation of the novel analogues as antivirals against HCV as well. The effects of the synthesized analogues on HCV RNA replication (Table 1, Figure 3) and cell viability (Table 1) were determined in the Huh5-2 stable cell line harboring the firefly luciferase-expressing subgenomic replicon of the HCV genotype 1b Con1 strain. The two most promising analogues

identified were **24** and **18**. These two compounds showed notable anti-HCV activity in 1b replicon cells, with half-maximal effective concentrations (EC<sub>50</sub>) of 10.5  $\mu$ M and 83.8  $\mu$ M, respectively (Figures 3 and 4), and promising safety since the median lethal concentrations (LC<sub>50</sub>) were higher than 200  $\mu$ M (the highest concentration tested). Compound **24** exhibited a significant selectivity index (SI>19.1, SI: LC<sub>50</sub>/EC<sub>50</sub>). The inhibition profiles measured by the luciferase assay were confirmed using indirect immunofluorescence against NS5A (Figure 5). Huh5-2 cells were treated for 7 days (2 passages), as the standard treatment used for luciferase measurement showed no significant reduction (data not shown), possibly because of the much higher half-life of NS5A<sup>58</sup> compared to the luciferase protein.



**Figure 3**. Evaluation of flutimide analogues against HCV genotype 1b RNA replication, as determined in Huh5-2 subgenomic replicon cells, seeded at 30% confluence and treated for 72 h with the compounds at a concentration of 100  $\mu$ M. As a marker of viral RNA replication, the firefly luciferase activity was measured and expressed as relative light units (RLU) per  $\mu$ g of total protein. Values of the

compound-treated cells were expressed as the percentage compared to mock (M)-treated cells that received the solvent (DMSO).

To gain insight to the interaction between the active compounds and the potential molecular target responsible for the observed antiviral effects, docking of the novel analogues in the active site of HCV polymerase was performed, utilizing the crystal structure of the HCV NS5B polymerase in complex with UTP<sup>35</sup> (pdb id: 1GX6). Docking showed that all compounds could be efficiently accommodated within the polymerase active site by chelating the two metal ions bound to residues Asp318, Asp319 and Asp220 through their diketopiperazine moiety and thus accounting for the fair bioactivity observed (Figure 6). The molecules were further stabilized through hydrophobic and Van der Waals interactions formed between the ligand and residues Leu159 and Phe224 and, moreover, by cation-π face-to-face and faceto-edge stacking interactions with the sidechains of Arg48 and Arg158, respectively. Interestingly, the predicted binding mode of the most active flutimide analogue 24 indicates that the hydrophobic cavity adjacent to the enzyme catalytic pocket (shown by a yellow arrow in Figure 6) can possibly accommodate specific interactions with substituents of position 8, thus facilitating future design of compounds with higher affinity and improved selectivity towards HCV NS5B polymerase. Although the theoretical results presented herein can be considered as a good indication that novel compounds could indeed target the HCV polymerase as well, the SAR trend cannot be fully validated on the basis of the experimentally available data and additional synthesis will be required in the case of HCV to definitely establish the molecular target of the novel derivatives.

## 18 - HCV Replication - Huh5-2

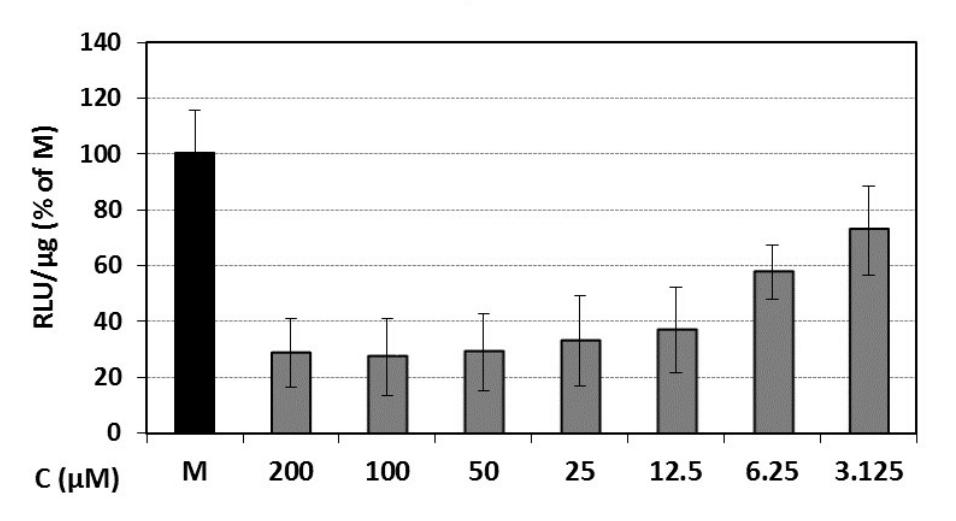


**Figure 4.** Confirmation of the anti-HCV activity of flutimide analogue **18** using 6-point dose-response curve analysis of 2-fold serial dilutions. The assay was done in Huh5-2 replicon cells. M = mock-treated control.

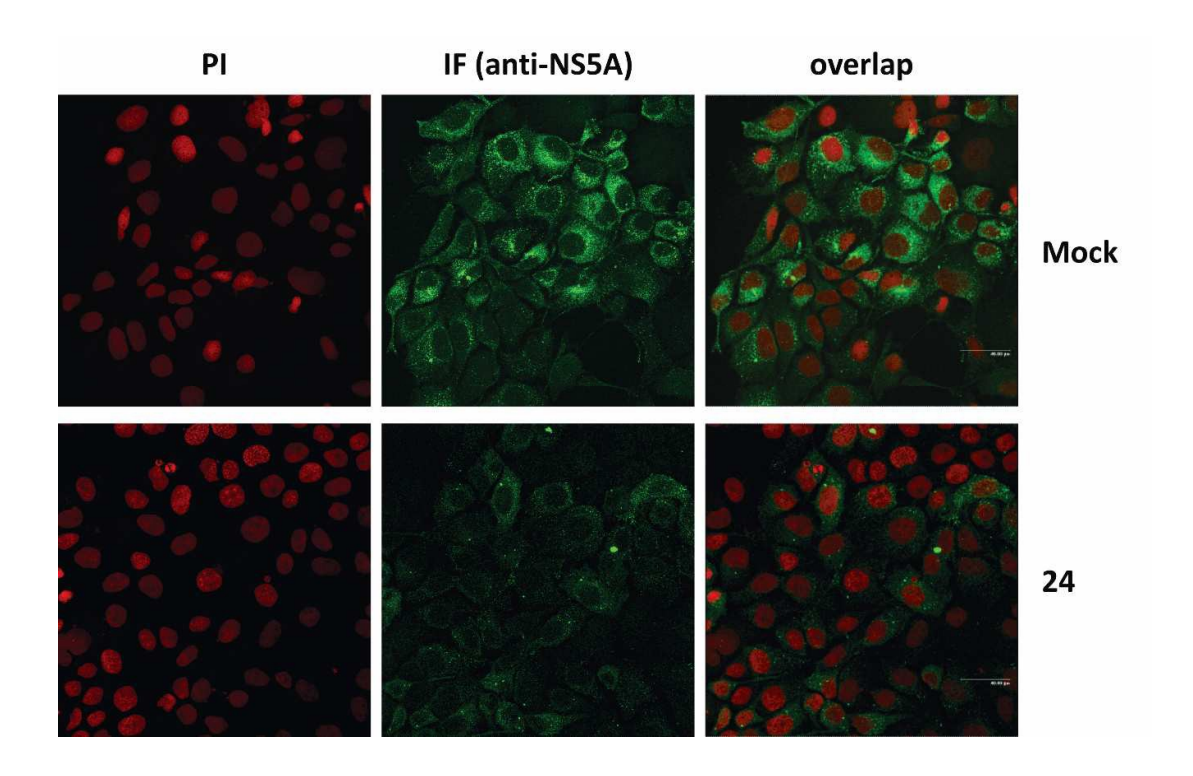
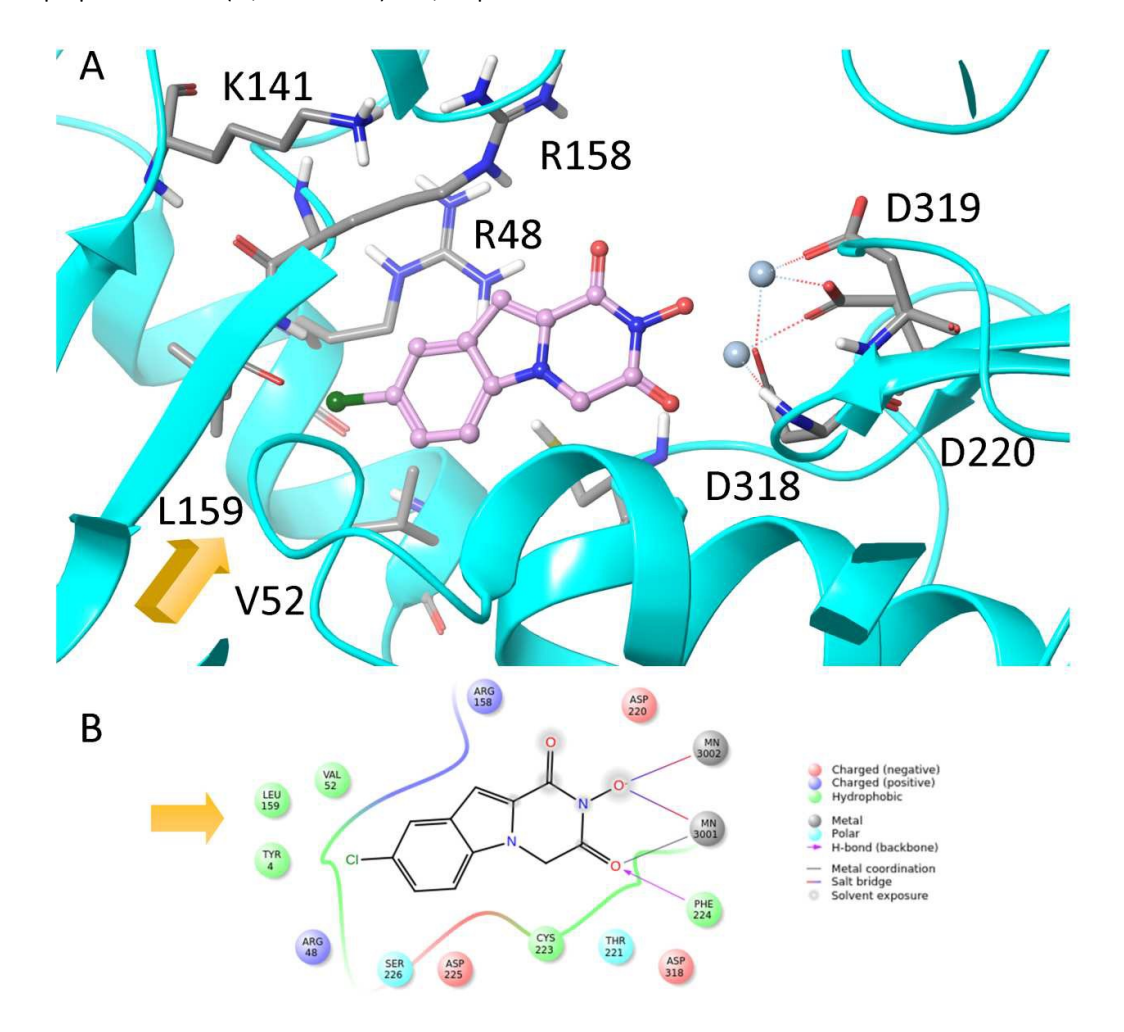


Figure 5. Inhibitory effect of 24 on HCV protein expression. Indirect immunofluorescence for NS5A in Huh5-2 replicon cells, treated with 24 at 100  $\mu$ M, or DMSO (Mock). Nuclei were stained with propidium iodide (PI; left column). Bar, 40  $\mu$ m.



**Figure 6**. A) The predicted binding orientation of the most active chloro-derivative **24** in the catalytic site of the HCV polymerase shown in a ribbon representation. The analogue efficiently chelates the two metal ions bound to residues Asp318, Asp319 and Asp220 through the diketopiperazine moiety and is further stabilized through hydrophobic interactions formed between the ligand and residues Leu159 and Phe224 as well as stacking interactions with sidechains of Arg48 and Arg158. Docking demonstrated the existence of a hydrophobic cavity adjacent to the enzyme catalytic pocket (shown by a yellow arrow) that can possibly offer specific interactions with substituents at positions 8 and 9 of the novel scaffold, thus facilitating rational design of compounds with higher affinity and improved

selectivity for the HCVC NS5B polymerase. B) Two-dimensional diagram of the interactions between the inhibitor and the polymerase active site.

## Conclusion

In summary, by incorporating the 2,6-diketopiperazine moiety of flutimide into the pharmacophore ring of indole, we have obtained compounds demonstrating potent inhibitory activity against influenza PA endonuclease, with  $IC_{50}$  values in the range of 13-29  $\mu$ M and more optimal drug-like properties compared to DPBA (Table 1, logD and p $K_a$ ). This activity was in perfect agreement with the predicted binding mode of the novel analogues. While the N-hydroxyimide group was predicted to chelate the two catalytic metal ions in the enzyme active site, the extended aromatic system of the analogues facilitated extensive stacking interactions with the protein and assisted the orientation of the various indole substitutions towards the hydrophobic cavity adjacent to the active site and a cluster of unstable water molecules bound within it. The biological studies showed that the most favorable indole substitution is fluorine at position 8 (compound 18).

In addition, the effect of the synthesized indole heterocycles on HCV replication and cell viability was determined. Two promising compounds, **24** and **18**, were identified, and **24** exhibited a remarkable selectivity index (>19). Interestingly, both of them bear an electron withdrawing group, chlorine and fluorine, respectively. This correlation was not noticed in the case of influenza virus PA endonuclease. Another interesting point arising from this report is that removal of the hydroxyl group from the imide nitrogen of our compounds (compound **26**)

caused a dramatic reduction in their potency against influenza endonuclease as well as HCV. This supports the critical role of the hydroxyl group in chelating the metal ions within the active center of the target enzymes.

Our findings suggest that the novel pyrazino[1,2-a]indole-1,3(2H,4H)-dione framework that we have developed, following mild and experimentally convenient protocols, offers a promising motif for further construction of new analogues with optimized antiviral properties through appropriate substitution in the diketopiperazine or indole ring nuclei. Future experiments should deliver more detailed SAR information to help refine the requirements for optimal antiviral activity.

## **Experimental**

## Chemistry

**General.** Melting points were determined using a Büchi capillary apparatus and are uncorrected. The 1H and 13C NMR spectra were obtained on either a Bruker MSL 400 (400 MHz  $^1$ H; 100 MHz  $^{13}$ C) or Bruker 600 (600 MHz  $^1$ H) spectrometer, using CDCl<sub>3</sub> or DMSO- $d_6$  as solvent. Chemical shifts are reported in  $\delta$  (ppm) with the tetramethylsilane or solvent (DMSO- $d_6$ ) as internal standard. Spliting paterns are designated as s, singlet; d, doublet; dd, doublet of doublets; t, triplet; td, triplet of doublets; q, quartet; m, multiplet; bs, broad singlet.. Coupling constants (J) are expressed in units of hertz (Hz). The spectra were recorded at 293 K (20  $^{\circ}$ C) unless otherwise specified. Carbon multiplicities were established by DEPT experiments. The 2D NMR experiments (HMQC, HMBC and COSY) were performed for the elucidation of the structures of the newly synthesized compounds. Analytical thin-layer chromatography (TLC) was conducted on precoated Merck silica gel 60 F254

plates (layer thickness 0.2 mm) with the spots visualized by iodine vapors and/or UV light. Column chromatography purification was carried out on silica gel 60 (0.040-0.063 mm). Elemental analyses (C, H, N) were performed by the Service Central de Microanalyse at CNRS (France), and were within ±0.4% of the theoretical values. Elemental analysis results for the tested compounds correspond to >95% purity. The commercial reagents were purchased from Alfa Aesar, Sigma-Aldrich, and Merck, and were used without further purification except for the benzyl bromoacetate. This reagent was purified by fractional distillation in vacuo prior to use. Organic solvents used were in the highest purity, and when necessary, were dried by the standard methods. Solvent abbreviations: THF, tetrahydrofuran; DMF, dimethylformamide; Et<sub>2</sub>O, diethyl ether; MeOH, methanol; EtOH, ethanol; AcOEt, ethyl acetate; DMSO, dimethylsulfoxide. Reagent abbreviations: DMAP, 4-(Dimethylamino)pyridine; DCC, *N,N'*-Dicyclohexylcarbodiimide; N-(3-Dimethylaminopropyl)-N'EDCI·HCI, ethylcarbodiimide hydrochloride; HOBt, 1-Hydroxybenzotriazole hydrate; DIEA, N,N-Diisopropylethylamine; TFA, trifluoroacetic acid.

## Synthesis of 4-methoxy-benzyl 5-chloro-1*H*-indole-2-carboxylate (20)

A solution of 5-chloro-1*H*-indole-2-carboxylic acid (5.0 g, 26.0 mmol), 4-methoxybenzyl alcohol (4.49 g, 32.5 mmol), and DMAP (640 mg, 5.24 mmol) in 162 mL of dichloromethane was treated with DCC (5.36, 26.0 mmol) and stirred at room temperature for 3 h. The resulting mixture was filtered, concentrated *in vacuo*, taken up in 250 mL of ethyl acetate, and filtered. The solution was subsequently washed sequentially with 1 N HCl (2x30 mL), H<sub>2</sub>O (2x30 mL), saturated aqueous solution of NaHCO<sub>3</sub> (2x50 mL), brine (2x35 mL), dried over Na<sub>2</sub>SO<sub>4</sub>, and concentrated *in vacuo*. The residue was purified by flash column chromatography, using a mixture of eluents

n-hexane/AcOEt (4:1), to afford 20 (5.04 g, 62%) as a pale yellow crystalline solid; mp 160-162 °C (AcOEt/n-pentane).

<sup>1</sup>H NMR (400 MHz, CDCl<sub>3</sub>) δ (ppm) 3.82 (s, 3H, OC*H*<sub>3</sub>), 5.33 (s, 2H, C*H*<sub>2</sub>), 6.92 (d, 2H, J=8.0 Hz,  $H_{3'}$ ,  $H_{5'}$ ), 7.17 (s, 1H,  $H_{3}$ ), 7.25 (d, 1H, J=8.5 Hz,  $H_{6}$ ), 7.31 (d, 1H, J=8.6 Hz,  $H_{7}$ ), 7.40 (d, 2H, J=8.1 Hz,  $H_{2'}$ ,  $H_{6'}$ ), 7.63 (s, 1H,  $H_{4}$ ), 9.14 (bs, 1H, N*H*); <sup>13</sup>C NMR (100 MHz, CDCl<sub>3</sub>) δ (ppm) 55.1 (OCH<sub>3</sub>), 66.2 (COO*C*H<sub>2</sub>Ph), 107.6 ( $C_{3}$ ), 113.5 ( $C_{7}$ ), 113.8 ( $C_{3'}$ ,  $C_{5'}$ ), 121.1 ( $C_{4}$ ), 125.1 ( $C_{6}$ ), 126.7 ( $C_{3a}$ ), 127.7 ( $C_{5}$ ), 127.9 ( $C_{1'}$ ), 128.5 ( $C_{2}$ ), 130.0 ( $C_{2'}$ ,  $C_{6'}$ ), 135.7 ( $C_{7a}$ ), 159.5 ( $C_{4'}$ ), 161.5 (C=0). Anal. Calcd for C<sub>17</sub>H<sub>14</sub>ClNO<sub>3</sub>: C, 64.67; H, 4.47; N, 4.44. Found C, 64.79; H, 4.53; N, 4.48.

## Synthesis of 4-methoxybenzyl-5-chloro-1-(2-ethoxy-2-oxoethyl)-1*H*-indole-2 carboxylate (21)

Sodium hydride (209 mg, 9.78 mmol, 60% in mineral oil was added portionwise to a stirred, ice-cold, solution of 4-methoxy-benzyl 5-chloro-1*H*-indole-2-carboxylate **20** (2.5 g, 7.92 mmol) in dry DMF (8 mL). After stirring at room temperature for 1 h under argon, ethyl bromoacetate (1.44 g, 8.62 mmol), dissolved in dry DMF (3 mL) was added dropwise. Stirring was continued at rt for 24 h under argon, and the reaction mixture was then poured onto ice/water mixture (80 mL), and extracted with AcOEt (4x60 mL). The combined organic extracts were washed with brine (3x25 mL), dried (Na<sub>2</sub>SO<sub>4</sub>), and evaporated *in vacuo*. The crude residue was purified flash by column chromatography on silica gel (CH<sub>2</sub>Cl<sub>2</sub>), to afford **21** (2.24 g, 70%) as a white crystalline solid; mp 112-114 °C (AcOEt/*n*-pentane, Et<sub>2</sub>O).

<sup>1</sup>H NMR (400 MHz, CDCl<sub>3</sub>) δ (ppm) 1.24 (t, 3H, J=7.1 Hz, COOCH<sub>2</sub>CH<sub>3</sub>), 3.82 (s, 3H, OCH<sub>3</sub>), 4.19 (q, 2H, J=7.1 Hz, COOCH<sub>2</sub>CH<sub>3</sub>), 5.27 (s, 2H, COOCH<sub>2</sub>Ph), 5.28 (s, 2H, NCH<sub>2</sub>COO), 6.92 (dd, 2H, J<sub>1</sub>=8.7 Hz, J<sub>2</sub>=2.1 Hz, H<sub>3</sub>′, H<sub>5</sub>′), 7.20 (d, 1H, J=8.9 Hz, H<sub>7</sub>), 7.25-

7.32 (m, 2H,  $H_3$ ,  $H_6$ ), 7.38 (dd, 2H,  $J_1$ =8.7 Hz,  $J_2$ =2.1 Hz,  $H_2$ ,  $H_6$ ), 7.63 (d, 1H, J=1.5 Hz,  $H_4$ ); <sup>13</sup>C NMR (100 MHz, CDCl<sub>3</sub>)  $\delta$  (ppm) 14.2 (CH<sub>2</sub>CH<sub>3</sub>), 46.4 (NCH<sub>2</sub>COOCH<sub>2</sub>CH<sub>3</sub>), 55.4 (OCH<sub>3</sub>), 61.7 (CH<sub>2</sub>CH<sub>3</sub>), 66.6 (COOCH<sub>2</sub>Ph), 110.8 ( $C_3$ ), 110.9 ( $C_7$ ), 114.1 ( $C_3$ ,  $C_5$ ), 122.1 ( $C_4$ ), 126.1 ( $C_6$ ), 126.9 ( $C_{3a}$ ), 127.1 ( $C_5$ ), 127.9 ( $C_1$ ), 128.8 ( $C_2$ ), 130.2 ( $C_2$ ,  $C_6$ ), 137.9 ( $C_{7a}$ ), 159.9 ( $C_4$ ), 161.8 (COOCH<sub>2</sub>Ph), 168.7 (COOCH<sub>2</sub>CH<sub>3</sub>). Anal. Calcd for C<sub>21</sub>H<sub>20</sub>CINO<sub>5</sub>: C, 62.77; H, 5.02; N, 3.49. Found: C, 62.63; H, 5.04; N, 3.35.

## Synthesis of 5-chloro-1-(2-ethoxy-2-oxoethyl)-1*H*-indole-2-carboxylic acid (22)

To a solution of 4-methoxybenzyl-5-chloro-1-(2-ethoxy-2-oxoethyl)-1*H*-indole-2-carboxylate **21** (200 mg, 0.49 mmol) and anisole (2.12 g, 19.6 mmol) in dry dichloromethane (4.2 mL) was added dropwise TFA (2 mL, 26.52 mmol) and the mixture was stirred for 3 h at 30 °C under argon. Evaporation of the solvents afforded **22** (130 mg, 94%) as a white crystalline solid; mp 190-192 °C (AcOEt/*n*-pentane, Et<sub>2</sub>O).

<sup>1</sup>H NMR (400 MHz, DMSO- $d_6$ ) δ (ppm) 1.19 (t, 3H, J=7.1 Hz, COOCH<sub>2</sub>CH<sub>3</sub>), 4.13 (q, 2H, J=7.1 Hz, COOCH<sub>2</sub>CH<sub>3</sub>), 5.38 (s, 2H, NCH<sub>2</sub>COO), 7.25 (s, 1H, H<sub>3</sub>), 7.32 (dd, 1H, J<sub>1</sub>=8.9 Hz, J<sub>2</sub>=2.1 Hz, H<sub>6</sub>), 7.69 (d, 1H, J=8.9 Hz, H<sub>7</sub>), 7.77 (s, 1H, J=2.0 Hz, H<sub>4</sub>), 13.24 (bs, 1H, COOH); <sup>13</sup>C NMR (100 MHz, DMSO-d<sub>6</sub>) δ (ppm) 14.1 (COOCH<sub>2</sub>CH<sub>3</sub>), 46.3 (NCH<sub>2</sub>COO), 60.8 (COOCH<sub>2</sub>CH<sub>3</sub>), 109.5 (C<sub>3</sub>), 112.6 (C<sub>7</sub>), 121.2 (C<sub>4</sub>), 124.8 (C<sub>6</sub>), 125.1 (C<sub>5</sub>), 126.4 (C<sub>3a</sub>), 129.7 (C<sub>2</sub>), 137.6 (C<sub>7a</sub>), 162.6 (COOH), 168.8 (COOCH<sub>2</sub>CH<sub>3</sub>). Anal. Calcd for C<sub>13</sub>H<sub>12</sub>CINO<sub>4</sub>: C, 55.43; H, 4.29; N, 4.97. Found: C, 55.28; H, 4.36; N, 4.99.

## Synthesis of 8-chloro-2-((4-methoxybenzyl)oxy)pyrazino[1,2- $\alpha$ ]indole-1,3(2H,4H)-dione (23)

To a solution of 5-chloro-1-(2-ethoxy-2-oxoethyl)-1H-indole-2-carboxylic acid **22** (150 mg, 0.53 mmol) in a mixture of CH<sub>2</sub>Cl<sub>2</sub>/DMF (4:1, 6 mL) were added sequentially

EDCI·HCI (121 mg, 0.63 mmol), HOBt (86 mg, 0.64 mmol), DIEA (171.2 mg, 1.33 mmol) and O-(4-methoxybenzyl)hydroxylamine (97.4 mg, 0.64 mmol) and the mixture was stirred at 35 °C for 48 h under argon. The reaction mixture was concentrated under reduced pressure, poured onto ice/water mixture (10 mL), and extracted with AcOEt (4x15 mL). The combined organic extracts were washed with water (4x10 mL), 10% aqueous solution of Na<sub>2</sub>CO<sub>3</sub> (2x10 mL), brine (3x10 mL), dried (Na<sub>2</sub>SO<sub>4</sub>), and evaporated *in vacuo*. The residue was purified through flash column chromatography on silica gel using a gradient solvent system starting from n-hexane/AcOEt (100:0) to n-hexane/AcOEt (0:100), to afford 23 (154 mg, 78%) as a white crystalline solid; mp 238-240 °C dec (AcOEt/n-pentane).

<sup>1</sup>H NMR (400 MHz, DMSO- $d_6$ ) δ (ppm) 3.78 (s, 3H, OC $H_3$ ), 5.00 (s, 2H, OC $H_2$ Ph), 5.35 (s, 2H,  $H_4$ ), 6.98 (d, 2H, J=8.4 Hz,  $H_{3'}$ ,  $H_{5'}$ ), 7.36 (s, 1H,  $H_{10}$ ), 7.43 (dd, 1H,  $J_1$ =8.9 Hz,  $J_2$ =1.4 Hz,  $H_7$ ), 7.50 (d, 2H, J=8.4 Hz,  $H_2$ ,  $H_{6'}$ ), 7.66 (d, 1H, J=8.9 Hz,  $H_6$ ), 7.86 (d, 1H, J=1.5 Hz,  $H_9$ ); <sup>13</sup>C NMR (100 MHz, DMSO- $d_6$ ) δ (ppm) 48.0 ( $C_4$ ), 55.1 (OCCH<sub>3</sub>), 77.5 (OCCH<sub>2</sub>Ph), 106.0 ( $C_{10}$ ), 113.1 ( $C_6$ ), 113.8 ( $C_{3'}$ ,  $C_{5'}$ ), 121.7 ( $C_9$ ), 125.6 ( $C_7$ ), 126.0 ( $C_{3a}$ ), 126.4 ( $C_5$ ), 127.0 ( $C_{10a}$ ), 127.5 ( $C_{1'}$ ), 131.3 ( $C_{2'}$ ,  $C_{6'}$ ), 135.0 ( $C_{5a}$ ), 155.2 ( $C_{4'}$ ), 159.8 ( $C_1$ =0), 163.1 ( $C_3$ =0). Anal. Calcd for  $C_{19}$ H<sub>15</sub>ClN<sub>2</sub>O<sub>4</sub>: C, 61.55; H, 4.08; Cl, 9.56; N, 7.56. Found: C, 61.66; H, 4.12; N, 7.62.

## Synthesis of 8-chloro-2-hydroxypyrazino[1,2- $\alpha$ ]indole-1,3(2H,4H)-dione (24)

To a solution of 8-chloro-2-((4-methoxybenzyl)oxy)pyrazino[1,2-a]indole-1,3(2H,4H)-dione **23** (200 mg, 0.54 mmol) and anisole (2.34 g, 21.6 mmol) in dry dichloromethane (15.2 mL) was added dropwise TFA (4 mL, 53.00 mmol) and the mixture was stirred for 3 h at 30 °C under argon. After removal of the solvents the crude residue was purified by flash column chromatography using a mixture of

eluents AcOEt/MeOH (5:1), to afford **24** (112 mg, 83%) as a pale yellow crystalline solid; mp 209-211 °C (dec, AcOEt, MeOH/*n*-pentane).

<sup>1</sup>H NMR (400 MHz, DMSO- $d_6$ ) δ (ppm) 5.34 (s, 2H,  $H_4$ ), 7.30 (s, 1H,  $H_{10}$ ), 7.40 (dd, 1H,  $J_1$ =8.8 Hz,  $J_2$ =1.0 Hz,  $H_7$ ), 7.63 (d, 1H, J=8.9 Hz,  $H_6$ ), 7.83 (s, 1H,  $H_9$ ), 10.71 (s, 1H, OH); <sup>13</sup>C NMR (100 MHz, DMSO- $d_6$ ) δ (ppm) 47.6 ( $C_4$ ), 105.5 ( $C_{10}$ ), 113.0 ( $C_6$ ), 121.6 ( $C_9$ ), 125.3 ( $C_7$ ), 125.9 ( $C_{9a}$ ), 127.0 ( $C_{10a}$ ), 127.5 ( $C_8$ ), 134.9 ( $C_{5a}$ ), 155.8 ( $C_1$ =O), 163.3 ( $C_3$ =O). Anal. Calcd for  $C_{11}H_7CIN_2O_3$ : C, 52.71; H, 2.82; N, 11.18. Found: C, 52.76; H, 2.83; N, 11.22.

#### References

- 1. Influenza (Seasonal), http://www.who.int/mediacentre/factsheets/fs211/en/index.html (accessed 3/5/2013).
- K. L. Nichol, J. Wuorenma and T. von Sternberg, Arch. Intern. Med. (Chic.), 1998, 158, 1769-1776.
- 3. C. Fytas, A. Kolocouris, G. Fytas, G. Zoidis, C. Valmas and C. F. Basler, *Bioorg. Chem.*, 2010, **38**, 247-251.
- 4. G. Zoidis, L. Naesens and E. De Clercq, Monatshefte für Chemie, 2013, 144, 515-521.
- 5. G. Zoidis, A. Tsotinis, N. Kolocouris, J. M. Kelly, S. R. Prathalingam, L. Naesens and E. De Clercq, *Org. Biomol. Chem.*, 2008, **6**, 3177-3185.
- M. D. de Jong, T. T. Tran, H. K. Truong, M. H. Vo, G. J. Smith, V. C. Nguyen, V. C. Bach, T. Q. Phan, Q. H. Do, Y. Guan, J. S. Peiris, T. H. Tran and J. Farrar, N. Engl. J. Med., 2005, 353, 2667-2672.
- S. K. Leang, Y. M. Deng, R. Shaw, N. Caldwell, P. Iannello, N. Komadina, P. Buchy, M. Chittaganpitch, D. E. Dwyer, P. Fagan, A. C. Gourinat, F. Hammill, P. F. Horwood, Q. S. Huang, P. K. Ip, L. Jennings, A. Kesson, T. Kok, J. L. Kool, A. Levy, C. Lin, K. Lindsay, O. Osman, G. Papadakis, F. Rahnamal, W. Rawlinson, C. Redden, J. Ridgway, I. C. Sam, S. Svobodova, A. Tandoc, G. Wickramasinghe, J. Williamson, N. Wilson, M. A. Yusof, A. Kelso, I. G. Barr and A. C. Hurt, *Antiviral Res.*, 2013, 97, 206-210.
- 8. S. J. Plotch, M. Bouloy, I. Ulmanen and R. M. Krug, *Cell*, 1981, **23**, 847-858.
- 9. A. Dias, D. Bouvier, T. Crepin, A. A. McCarthy, D. J. Hart, F. Baudin, S. Cusack and R. W. Ruigrok, *Nature*, 2009, **458**, 914-918.
- 10. P. Yuan, M. Bartlam, Z. Lou, S. Chen, J. Zhou, X. He, Z. Lv, R. Ge, X. Li, T. Deng, E. Fodor, Z. Rao and Y. Liu, *Nature*, 2009, **458**, 909-913.
- 11. K. Das, J. M. Aramini, L. C. Ma, R. M. Krug and E. Arnold, *Nat. Struct. Mol. Biol.*, 2010, **17**, 530-538.
- 12. A. Moscona, N. Engl. J. Med., 2009, **360**, 953-956.
- 13. M. Nakazawa, S. E. Kadowaki, I. Watanabe, Y. Kadowaki, M. Takei and H. Fukuda, *Antiviral Res.*, 2008, **78**, 194-201.
- 14. J. H. Hoofnagle, *Hepatology*, 2002, **36**, S21-29.
- 15. J. Wilder and K. Patel, N. A. J. Med. Sci., 2014, **7**, 1-7.

- 16. World Health Organization, Hepatitis C, http://www.who.int/mediacentre/factsheets/fs164/en/, (accessed 20/9/2015).
- 17. C. Zingaretti, R. De Francesco and S. Abrignani, *Clin. Microbiol. Infect.*, 2014, **20**, 103-109.
- 18. N. Arnaud, S. Dabo, P. Maillard, A. Budkowska, K. I. Kalliampakou, P. Mavromara, D. Garcin, J. Hugon, A. Gatignol, D. Akazawa, T. Wakita and E. F. Meurs, *PLoS One*, 2010, **5**, e10575.
- 19. U. A. Ashfaq, S. N. Khan, Z. Nawaz and S. Riazuddin, Genet Vaccines Ther, 2011, 9, 7.
- 20. C. Bain, P. Parroche, J. P. Lavergne, B. Duverger, C. Vieux, V. Dubois, F. Komurian-Pradel, C. Trepo, L. Gebuhrer, G. Paranhos-Baccala, F. Penin and G. Inchauspe, *J Virol*, 2004, **78**, 10460-10469.
- 21. V. Soriano, M. G. Peters and S. Zeuzem, Clin. Infect. Dis., 2009, 48, 313-320.
- T. Wakita, T. Pietschmann, T. Kato, T. Date, M. Miyamoto, Z. Zhao, K. Murthy, A. Habermann, H. G. Kräusslich, M. Mizokami, R. Bartenschlager and T. J. Liang, *Nat. Med.*, 2005, 11, 791-796.
- T. Burckstummer, M. Kriegs, J. Lupberger, E. K. Pauli, S. Schmittel and E. Hildt, FEBS Lett, 2006, 580, 575-580.
- 24. I. Barrera, D. Schuppli, J. M. Sogo and H. Weber, *J Mol Biol*, 1993, **232**, 512-521.
- 25. R. Bartenschlager, M. Frese and T. Pietschmann, Adv Virus Res, 2004, 63, 71-180.
- 26. N. Calland, J. Dubuisson, Y. Rouille and K. Seron, *Viruses*, 2012, **4**, 2197-2217.
- 27. M. Hattori, C. M. Ma, Y. Wei, R. S. El Dine and N. Sato, *Canadian Chemical Transactions*, 2013, **1**, 116-140.
- 28. A. M. Q. King, in *Virus Taxonomy*, eds. A. M. Q. King, M. J. Adams, E. B. Carstens and E. J. Lefkowitz, Elsevier, San Diego, 2012, DOI: <a href="http://dx.doi.org/10.1016/B978-0-12-384684-6.00086-0">http://dx.doi.org/10.1016/B978-0-12-384684-6.00086-0</a>, pp. 1003-1020.
- 29. P. Simmonds, J. Bukh, C. Combet, G. Deléage, N. Enomoto, S. Feinstone, P. Halfon, G. Inchauspé, C. Kuiken, G. Maertens, M. Mizokami, D. G. Murphy, H. Okamoto, J. M. Pawlotsky, F. Penin, E. Sablon, T. Shin-I, L. J. Stuyver, H. J. Thiel, S. Viazov, A. J. Weiner and A. Widell, *Hepatology*, 2005, **42**, 962-973.
- 30. R. Bartenschlager, V. Lohmann and F. Penin, Nat. Rev. Microbiol., 2013, 11, 482-496.
- 31. D. Moradpour, F. Penin and C. M. Rice, *Nat. Rev. Microbiol.*, 2007, **5**, 453-463.
- 32. C. T. Ranjith-Kumar and C. C. Kao, in *Hepatitis C Viruses: Genomes and Molecular Biology*, ed. S. L. Tan, Norfolk (UK), 2006.
- 33. C. A. Lesburg, M. B. Cable, E. Ferrari, Z. Hong, A. F. Mannarino and P. C. Weber, *Nat. Struct. Biol.*, 1999, **6**, 937-943.
- 34. S. Bressanelli, L. Tomei, A. Roussel, I. Incitti, R. L. Vitale, M. Mathieu, R. De Francesco and F. A. Rey, *Proc. Natl. Acad. Sci. U. S. A.*, 1999, **96**, 13034-13039.
- 35. S. Bressanelli, L. Tomei, F. A. Rey and R. De Francesco, *J. Virol.*, 2002, **76**, 3482-3492.
- 36. H. Ago, T. Adachi, A. Yoshida, M. Yamamoto, N. Habuka, K. Yatsunami and M. Miyano, *Structure*, 1999, **7**, 1417-1426.
- 37. J. Varshney, P. K. Sharma and A. Sharma, *Eur. Rev. Med. Pharmacol. Sci.*, 2012, **16**, 667-671.
- 38. D. Rogolino, M. Carcelli, M. Sechi and N. Neamati, *Coord. Chem. Rev.*, 2012, **256**, 3063-3086.
- J. E. Tomassini, M. E. Davies, J. C. Hastings, R. Lingham, M. Mojena, S. L. Raghoobar,
   S. B. Singh, J. S. Tkacz and M. A. Goetz, *Antimicrob. Agents Chemother.*, 1996, 40, 1189-1193.
- J. E. Tomassini, H. Selnick, M. E. Davies, M. E. Armstrong, J. Baldwin, M. Bourgeois, J. Hastings, D. Hazuda, J. Lewis, W. McClements, G. Ponticello, E. Radzilowski, G. Smith, A. Tebben and A. Wolfe, *Antimicrob. Agents Chemother.*, 1994, 38, 2827-2837.

- 41. E. Kowalinski, C. Zubieta, A. Wolkerstorfer, O. H. Szolar, R. W. Ruigrok and S. Cusack, *PLoS Pathog.*, 2012, **8**, e1002831.
- 42. J. Q. Hang, S. Rajendran, Y. Yang, Y. Li, P. W. In, H. Overton, K. E. Parkes, N. Cammack, J. A. Martin and K. Klumpp, *Biochem. Biophys. Res. Commun.*, 2004, **317**, 321-329.
- 43. V. Suchaud, F. Bailly, C. Lion, C. Calmels, M. L. Andreola, F. Christ, Z. Debyser and P. Cotelle, *J. Med. Chem.*, 2014, **57**, 4640-4660.
- 44. I. Bougie, S. Charpentier and M. Bisaillon, *J. Biol. Chem.*, 2003, **278**, 3868-3875.
- 45. A. Stevaert, S. Nurra, N. Pala, M. Carcelli, D. Rogolino, C. Shepard, R. A. Domaoal, B. Kim, M. Alfonso-Prieto, S. A. Marras, M. Sechi and L. Naesens, *Mol. Pharmacol.*, 2015, **87**, 323-337.
- 46. C. Cianci, T. D. Y. Chung, N. Meanwell, H. Putz, M. Hagen, R. J. Colonno and M. Krystal, *Antivir. Chem. Chemother.*, 1996, **7**, 353-360.
- 47. K. E. Parkes, P. Ermert, J. Fässler, J. Ives, J. A. Martin, J. H. Merrett, D. Obrecht, G. Williams and K. Klumpp, *J. Med. Chem.*, 2003, **46**, 1153-1164.
- 48. M. Z. Zhang, Q. Chen and G. F. Yang, Eur. J. Med. Chem., 2015, **89**, 421-441.
- 49. H. Y. Sagong, A. Parhi, J. D. Bauman, D. Patel, R. S. Vijayan, K. Das, E. Arnold and E. J. LaVoie, *ACS Med. Chem. Lett.*, 2013, **4**, 547-550.
- 50. A. K. Parhi, A. Xiang, J. D. Bauman, D. Patel, R. S. Vijayan, K. Das, E. Arnold and E. J. Lavoie, *Biorg. Med. Chem.*, 2013, **21**, 6435-6446.
- 51. SZMAP 1.2.1.4: OpenEye Scientific Software, Santa Fe, NM., http://www.eyesopen.com, (accessed 25/9/2015).
- 52. R. A. Friesner, J. L. Banks, R. B. Murphy, T. A. Halgren, J. J. Klicic, D. T. Mainz, M. P. Repasky, E. H. Knoll, M. Shelley, J. K. Perry, D. E. Shaw, P. Francis and P. S. Shenkin, *J. Med. Chem.*, 2004, **47**, 1739-1749.
- 53. R. A. Friesner, R. B. Murphy, M. P. Repasky, L. L. Frye, J. R. Greenwood, T. A. Halgren, P. C. Sanschagrin and D. T. Mainz, *J. Med. Chem.*, 2006, **49**, 6177-6196.
- 54. T. A. Halgren, R. B. Murphy, R. A. Friesner, H. S. Beard, L. L. Frye, W. T. Pollard and J. L. Banks, *J. Med. Chem.*, 2004, **47**, 1750-1759.
- 55. A. J. Brooks, J. S. Hammond, K. Girling and I. J. Beckingham, *J Surg Res*, 2007, **141**, 247-251.
- 56. D. J. Kempf and S. L. Condon, The Journal of Organic Chemistry, 1990, 55, 1390-1394.
- 57. A. Stevaert, R. Dallocchio, A. Dessì, N. Pala, D. Rogolino, M. Sechi and L. Naesens, *J. Virol.*, 2013, **87**, 10524-10538.
- 58. T. Pietschmann, V. Lohmann, G. Rutter, K. Kurpanek and R. Bartenschlager, *J Virol*, 2001, **75**, 1252-1264.